Advances in Geosciences

Sahara dust, ocean spray, volcanoes, biomass burning: pathways of nutrients into Andean rainforests

P. Fabian[1], R. Rollenbeck[1,2], N. Spichtinger[1], L. Brothers[3], G. Dominguez[3], and M. Thiemens[3]

[1]Technical University of Munich (TUM), TUM Life Science Center Weihenstephan, Am Hochanger 13, 85354 Freising, Germany
[2]Laboratory for Climatology and Remote Sensing (LCRS), University of Marburg, Germany
[3]Department of Chemistry, University of California San Diego (UCSD), USA

Abstract. Regular rain and fogwater sampling in the Podocarpus National Park, on the humid eastern slopes of the Ecuadorian Andes, along an altitude profile between 1960 and 3180 m, has been carried out since 2002. The samples, accumulated over about 1-week intervals, were analysed for pH, conductivity and major ions (K^+, Na^+, NH_4^+, Ca^{2+}, Mg^{2+}, Cl^-, SO_4^{2-}, NO_3^-, PO_4^{3-}).

About 35% of the weekly samples had very low ion contents, with pH mostly above 5 and conductivity below $10\,\mu$S/cm. 10-days back trajectories (FLEXTRA) showed that respective air masses originated in pristine continental areas, with little or no obvious pollution sources.

About 65%, however, were significantly loaded with cations and anions, with pH as low as 3.5 to 4.0 and conductivity up to $50\,\mu$S/cm. The corresponding back trajectories clearly showed that air masses had passed over areas of intense biomass burning, active volcanoes, and the ocean, with episodic Sahara and/or Namib desert dust interference.

Enhanced SO_4^{2-} and NO_3^+ were identified, by combining satellite-based fire pixel observations with back trajectories, as predominantly resulting from biomass burning. Analyses of oxygen isotopes ^{16}O, ^{17}O, and ^{18}O in nitrate show that nitrate in the samples is indeed a product of atmospheric conversion of precursors. Some SO_4^{2-}, about 10% of the total input, could be identified to originate from active volcanoes, whose plumes were encountered by about 10% of all trajectories.

Enhanced Na^+, K^+, and Cl^- were found to originate from ocean spray sources. They were associated with winds providing Atlantic air masses to the receptor site within less than 5 days. Episodes of enhanced Ca^{2+} and Mg^{2+} were found to be associated with air masses from African deserts. Satellite aerosol data confirm desert sources both on the Northern (Sahara) as on the Southern Hemisphere (Namib), depending on the season. A few significant PO_4^{3-} peaks are related with air masses originating from North African phosphate mining fields.

1 Introduction

The role of long-range transport of nutrients to remote ecosystems has been documented by a variety of scientific articles.

Saharan dust is considered to be the main source of mineral ions that fertilize the Amazon basin (Talbot et al., 1990; Formenti et al., 2001; Koren et al., 2006).Base metals such as Ca and Mg which are important for controlling key plant functions, are particularly low in Amazonian ecosystems due to highly weathered soils and the absence of local base metal sources (Cuevas and Medina, 1986, 1988). They are carried in by Saharan dust featuring a remarkable arrangement in nature, in which most of the mineral dust arriving in the Amazon basin originates from a single source of only 0.5% the size of the Amazon, the Bodélé depression located northeast of Lake Chad (Koren et al., 2006). Boy and Wilcke (2008) have speculated whether Saharan dust can be carried even further and traverse the humid Amazon basin towards the

Andes. They clearly show that Ca and Mg in rainwater fertilizing the mountaineous rain forest on the eastern slopes of the Ecuadorian Andes (the research site of this study) does indeed originate from Saharan dust.

Biomass burning is a source of carbon, sulfur and nitrogen compounds, which, along with their photochemically generated reaction products, can be transported over very long distances, even traversing oceans.

Besides CO_2, a large array of chemical species is emitted from burning forests, such as carbon monoxide, hydrocarbons, halocarbons, SO_2, COS, NO_x, HCN, and aerosols (see Crutzen and Andreae, 1990; Andreae and Merlet, 2001 and the references given therein). In the plume, secondary substances such as ozone are produced photochemically (Fujiwara et al., 1999; Marufu et al., 2000). Likewise, the reactive sulphur and nitrogen compounds are converted to sulphate and nitrate, respectively, which are soluble in cloud droplets (Chang et al., 1987).Although scavenging by rain is considered fast, with atmospheric residence times of SO_2^{2-} and NO_3^- of about 2 days only, recent investigations in Brazil (Andreae et al., 2004 and Koren et al., 2004) show that heavy smoke from fires reduces cloud drop sizes, thus causing suppression of low-level rainout, allowing transport to higher levels and thus over larger distances. In an earlier study Fabian et al. (2005) demonstrated that sulphate and nitrate originating from biomass burning in the Amazon is fertilizing the Andean rain forest of Ecuador.

Products of tropical biomass burning have been found over the Atlantic and Pacific oceans (Roelofs et al., 1997; Andreae et al., 2001), forest fire emissions from Siberia and Canada have been identified in Japan (Tanimoto et al., 2000) and Europe (Spichtinger et al., 2001), respectively, and forest fire smoke from Russia has even made it around the world (Damoah et al., 2003).

High sulphate deposition rates have also been observed in montane tropical rain forests of Costa Rica, Colombia and Puerto Rico (Clark et al., 1998; Veneklaas, 1990; Ashbury et al., 1994), respectively, but these were largely due to maritime air masses and volcanic activity in the vicinity.

Tracers of sea salt emissions are, besides sulfur compounds, Na^+, K^+, and Cl^-, which have been widely observed in the Amazon (Andreae et al., 1990; Formenti et al., 2001). K^+ and Cl^- have also been found in biogenic aerosol (Artaxo et al., 1990).

In this paper we report on ions analysed in rain and fogwater samples collected on the eastern slopes of the Ecuadorian Andes, which show the importance of long-range transport and the impact of desert dust, ocean spray, biomass burning and volcanism on the nutrient supply of the mountain forest ecosystem. If sustained for longer periods, these additions to the nutrient balance may have the potential to alter the natural composition of the ecosystem.
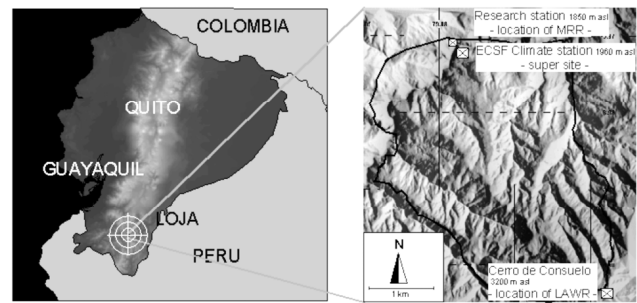

Fig. 1. Map showing the research area in Ecuador.

2 Data collection and analyses

Regular rain and fogwater sampling in the Podocarpus National Park, along an altitude profile between 1960 and 3180 m, has been carried out since 2002. The research area is located in southern Ecuador, on the humid eastern slopes of the Andes, bordered by the Rio San Francisco and dominated by winds from easterly directions. The research site is depicted in Fig. 1.

Precipitation rates vary with the annual variation of the trade wind system, with highest rainfall during April–July and a short dry period in October–November. The forced orographic ascent of warm and moist air masses originating in the Amazon lowlands leads to regular and intense cloud formation resulting in considerable fog water input into the ecosystem. The fog water fraction of the total water input, which varies between about 2500 and 7000 mm/year over the observed altitude range, increases from about 5% at 1960 m to 30% at 3180 m. One of the sampling sites (ECSF) with commercial rain collectors and fog collectors according to Schemenauer and Cereceda (1994) is shown in Fig. 2 (for details about rain and fog measurement techniques, calibration and data handling see Rollenbeck et al., 2007; Fabian et al., 2005; Rollenbeck and Bendix, 2006).

Rain and fogwater samples were collected in almost regular weekly intervals, but the amount of water was monitored with daily resolution, which allows to determine the daily contributions to the total sample. The stations which have been operating continuously since 2002 are listed in Table 1. While the first three of these span a height profile in the research area, El Tiro lies about 5 km downwind on a mountain pass.

All samples were analysed at TUM-WZW for pH (Methron 73065/682), conductivity (WTW-LF 90) and major ions (K^+, Na^+, NH_4^+, Ca^{2+}, Mg^{2+}, Cl^-, SO_4^{2-}, NO_3^-, PO_4^{3-}). Cation analyses were carried out by the inductivity-coupled plasma method (Perkin Elmer Optima 3000), while anions were analysed by ion chromatography (Dionex DX-210).

Every sample was analysed only once. Repeated analysis was performed only with samples whose ion contents

Fig. 2. ECSF climate station with rain and fogwater samplers.

Fig. 3. Ion concentration plots for NO_3, NH_4, and SO_4 analysed from weekly fogwater samples collected at El Tiro.

Table 1. Stations for rain and fogwater collection.

	Station	Altitude (m a.s.l.)
1	ECSF	1960
2	TSI	2660
3	Antenas	3180
4	El Tiro	2825

appeared suspicious. Thus no statistical errors can be given. We assume that the uncertainty of the results is of the order of the respective detection limit. The detection limits for the ions of interest here are compiled in Table 2.

3 Results and discussion

For all components strong variations are observed. pH and conductivity vary between lowest (highest) values of 4.0 and 40 μS/l, predominantly during November to April and highest (lowest) values of 5.8 and about 2 μS/l, respectively, mostly found during April to July.

From all samples collected between 2002 and 2006 we calculated annual averages (precipitation, pH and conductivity) and annual average deposition rates, respectively, for both rain and fog, as compiled in Table 3.

The fog contribution increases from low values at the lowermost station ECSF to 1600 mm/year at the top (Antenas), which is about 30% of the total precipitation there. Fogwater generally was found to show lower pH and higher conductivity than rainwater. Average annual ion deposition rates obtained by simply averaging over deposition rates of the 4 stations are shown in Sect. A of Table 3.

To obtain the total areal deposition, the observed values for the three stations were assigned to the altitude range they represent. The fractions of the respective altitude ranges were used as weighting factors for summing up total deposition. The altitude ranges of ECSF, TS1 and Antenas represent 0.42, 0.46, and 0.12, respectively, of the total research area. Respective deposition rates are shown in Sect. B of Table 3.

Station 4 (El Tiro) is special in being located about 5 km apart on a mountain pass downwind of the research area, surrounded by higher elevations leading to a funnel effect. In fact ion concentrations and deposition rates are very similar to the corresponding averages of stations 1–3. We conclude that El Tiro is the station which represents the average ion
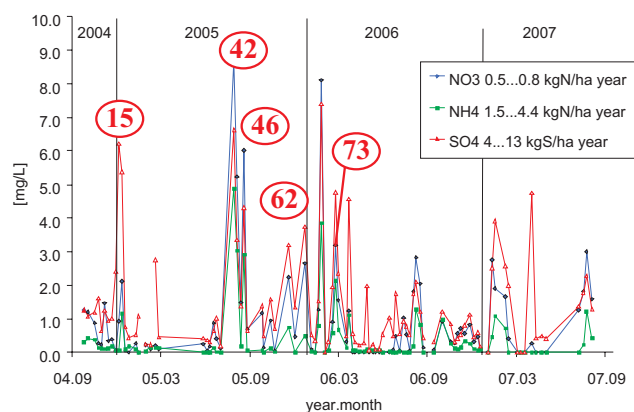
deposition of this area best. In the following study we therefore confine ourselves to data measured at El Tiro. In order to get continuous deposition data throughout the entire year including the dry period when rain is low or even absent, we concentrate on fog water data which are available during the dry period as well.

Time series of ions analysed from weekly fogwater samples at El Tiro are shown in Figs. 3–5 covering about 3 years, from October 2004 to September 2007. Two data gaps are noticeable, April/May of 2005 and February of 2007, due to logistic problems. Otherwise the data series represents a fairly complete set of almost regular weekly samples. The ions are grouped into NO_3, NH_4 and SO_4 (Fig. 3), Na, Cl and K (Fig. 4) and Ca, Mg, and PO_4 (Fig. 5) as discussed below.

3.1 NO_3, NH_4 and SO_4 (Fig. 3)

About 35% of the samples show very low ion values, of all 3 species, at or close to the detection limits. Corresponding pH values were above 5.0, conductivity below 10 μS/cm. Back trajectory analyses using the FLEXTRA model (Stohl and Wotawa, 1995) showed that these samples were dominated by air masses which mostly originated from pristine continental areas with little or no obvious pollution sources. About 65% of the weekly samples show distinct ion peaks, generally seen in all 3 species. For these samples the pH

Table 2. Detection limits of the different ions in mg/l.

Ion	Ca^{2+}	K^+	Mg^{2+}	Na^+	NO_3^-	SO_4^{2-}	PO_4^{3-}	Cl^-	NH_4^+
Detection limit	0.05	0.05	0.05	0.1	0.2	0.2	0.5	0.2	0.1

Table 3. Average annual precipitation (mm), pH, conductivity (μS/cm), and ion deposition rates (kg/ha) 2002–2006.

Station	water (mm)	pH	Conductiv.	NH_4	Ca	Cl	PO_4	Mg	NO_3	K	Na	SO_4
Rain input												
1. ECSF	1784	5.3	3.8	1.2	3.0	7.9	1.1	0.6	1.2	2.1	4.3	4.6
2. TSI	3861	5.3	2.8	2.7	3.6	13.3	2.2	0.9	2.0	3.5	7.3	9.0
3. Anten.	4353	5.2	3.1	3.0	4.1	13.6	1.8	1.3	3.1	3.1	7.8	8.9
4. El Tiro	1802	5.5	3.9	1.4	2.5	5.5	1.1	0.6	1.8	2.1	3.0	4.8
Fog input												
1. ECSF	131	5.0	6.2	0.2	0.3	0.7	0.1	0.1	0.2	0.2	0.3	0.6
2. TSI	495	5.1	6.1	0.7	0.7	1.9	0.6	0.2	0.7	0.5	1.0	2.2
3. Anten.	1604	4.9	12.0	7.7	2.4	6.2	2.0	0.7	11.0	1.9	3.7	14.5
4. El Tiro	941	4.8	21.6	4.1	1.2	3.8	1.1	0.5	7.8	1.6	2.4	11.9
A Average ion deposition stations 1–4												
Rain only				2.1	3.3	10.1	1.6	0.9	2.0	2.7	5.6	6.8
Fog only				3.2	1.2	3.2	1.0	0.4	4.9	1.1	1.9	7.3
TOTAL				5.3	4.5	13.3	2.6	1.3	6.9	3.8	7.5	14.1
B Average ion deposition stations 1–3 with area weighted factors												
Rain only				2.1	3.4	11.1	1.7	0.8	1.8	2.9	6.1	7.1
Fog only				1.3	0.7	1.9	0.6	0.2	1.7	0.5	1.0	3.0
TOTAL				3.4	4.1	13.0	2.3	1.0	3.5	3.4	7.1	10.1
C Average ion deposition station 4 (El Tiro)												
Rain only				1.4	2.5	5.5	1.1	0.6	1.8	2.1	3.0	4.8
Fog only				4.1	1.2	3.8	1.1	0.5	7.8	1.6	2.4	11.9
TOTAL				5.5	3.7	9.3	2.2	1.1	9.6	3.7	5.4	16.7

values were found as low as 3.5–4.0, and conductivity as high as 50 μS/cm. Five of the major ion peaks are marked by numbers. These will be discussed separately, with back trajectories showing the origin of the respective air masses.

NO_3, NH_4 and SO_4 ion concentrations are highly correlated indicating that all three are likely to originate from common sources. Figure 6 shows correlation plots of normalized NO_3/SO_4 and NO_3/NH_4 (left part), with Pearson correlation coefficients as high as 0.93 and 0.96, respectively. The red data point in the SO_4/NO_3 plot marks the weekly sample collected on 12 November, 2002, whose high SO_4 content was found to be due to the plume of the newly erupted Reventador volcanoe.

In an earlier paper (Fabian et al., 2005) we had shown that the common source of NO_3 and SO_4 ions in precipitation is largely biomass burning, with some contributions of volcanoes to SO_4. This conclusion was based on back trajectories combined with fire pixels detected by NOAA satellites.

14 of the earlier fogwater samples collected at El Tiro (October 2004 until August 2005), with significant NO_3, were analysed for oxygen isotope fractionation in NO_3. Interestingly, 10 of these show a mass independent fractionation and lie in the region of "Atmospheric nitrate" shown in the triple-isotope plot in Fig. 7. This characteristic deviation from the terrestrial mass dependent fractionation line is due to the fact that the formation of nitrate in the atmosphere requires ozone which has a mass independent fractionation of about 25 permille (Thiemens, 2006). From the fact that nitrate in
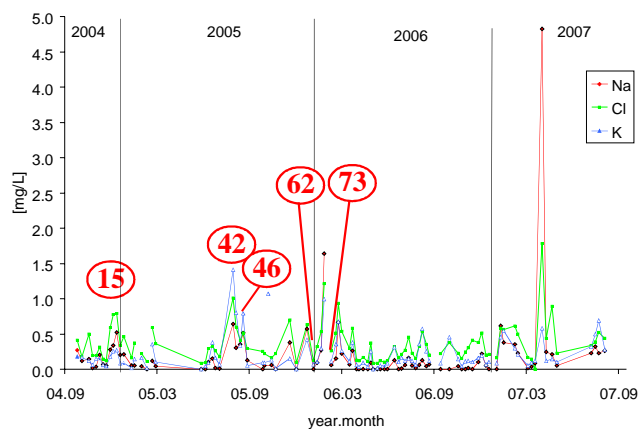
Fig. 4. Same as in Fig. 3, but for Na, Cl, and K.

Fig. 5. Same as in Fig. 3, but for Ca, Mg, and PO_4.

10 out of 14 fogwater samples shows the typical fractionation of "atmospheric nitrate" we can conclude that this nitrate was indeed formed photochemically in the atmosphere from precursor substances. It cannot be distinguished, however, between precursors due to biomass burning or other precursor sources such as air pollution, but the study by Boy et al. (2007) underlines the significance of this type of human activity to the emissions from Amazonia.

Four of the fogwater samples show different isotope behaviour, however. They lie close to the mass independent fractionation line and are marked "unknown nitrate source". At present we cannot offer a plausible interpretation for this effect.

In addition to the fogwater samples, 5 water samples from the river which is fed from the catchments of the research area, were analysed for isotope fractionation of their nitrate contents. As can be seen in Fig. 7, four of these lie correctly in the area marked "microbial nitrate" showing low values determined by OH in the biological system. One river sample, however, deviates and shows high isotope values close to the region of the "unknown nitrate source". We cannot offer a plausible interpretation of this deviation either. More systematic isotope analyses are under way to shed more light on these findings.

Some of the back trajectories were found to encounter plumes of active volcanoes. These are Tungurahua (1.467° S, 78.442° W), Sangay (2.002° S, 78.341° W), and Reventador (0.077° S, 77.656° W), all of them located in Ecuador. They have mostly been active throughout the time span discussed here. Figure 8 shows two 10-days back trajectories related to sample # 15 collected 20–26 December, 2004. Back trajectories are shown for 23 and 26 December only, which are the days which contribute more than 50% of the entire weekly fog sample.

Peak #15 shows the signatures of biomass burning, as indicated by the red fire pixels encountered by the 10-days back trajectories (Fig. 8). The high SO_4 peak points to significant additional sulfur from volcanic sources.
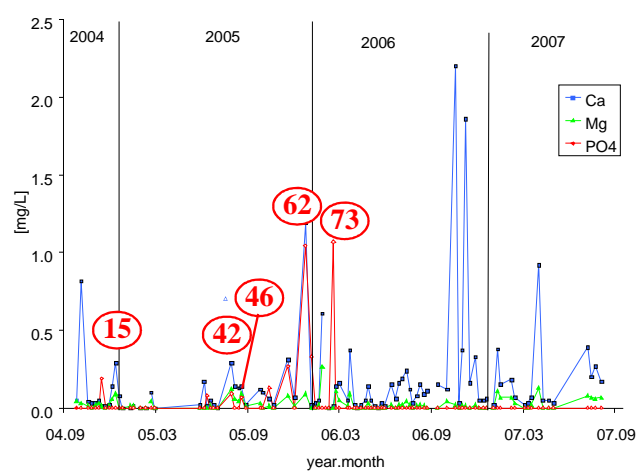
For 2005 and 2006 we determined those daily back trajectories which had passed at least over one of these volcanoes. We thereby considered a "width" of the trajectories of ±50 km, which is the resolution of the underlying global ECMWF model (European Center for Midrange Weather Forecast). For 2005 a total of 49 trajectories, and for 2006 33 trajectories were thus detected to pass the afore mentioned volcanoes. This is about 10% of all daily trajectories on average. We therefore conclude that about 10% of the SO_4 deposited at our research site originates, on average, from active volcanoes.

NH_4 is not an obvious product of biomass burning, although Graham et al. (2003) point out the biogenic origin of this species. The close correlation of NH_4 with NO_3 (Fig. 6) is, however, a strong argument for NH_4 being mainly related to biomass burning.

3.2 Na, Cl, and K (Fig. 4)

In Fig. 4 ion concentrations of Na, Cl, and K as analysed from El Tiro weekly fogwater samples, for the same 3-years sampling time as in Fig. 3 are shown. A similar behaviour as discussed before for the ions shown in Fig. 3 is noticeable. The five characteristic ion peaks are marked by numbers. The extreme Na peak occuring in 2007 is most likely an artefact due to contamination of the sample.

The obvious correlation of these ions which is quantified by Pearson correlation coefficients of 0.90 and 0.93 for Na/Cl and K/Cl, respectively (see Fig. 6) points to common sources of these species. As was evaluated by Andreae et al. (1990) and Formenti et al. (2001) already, ocean spray, i.e. sea salt aerosol is this common source.

10-days back trajectories related to samples # 42, 46, 62, and 73 as plotted in the Figs. 9–12 show the oceanic origin of air masses contributing to the high values of Na, Cl, and K found in these samples. As in Fig. 8, we plotted the
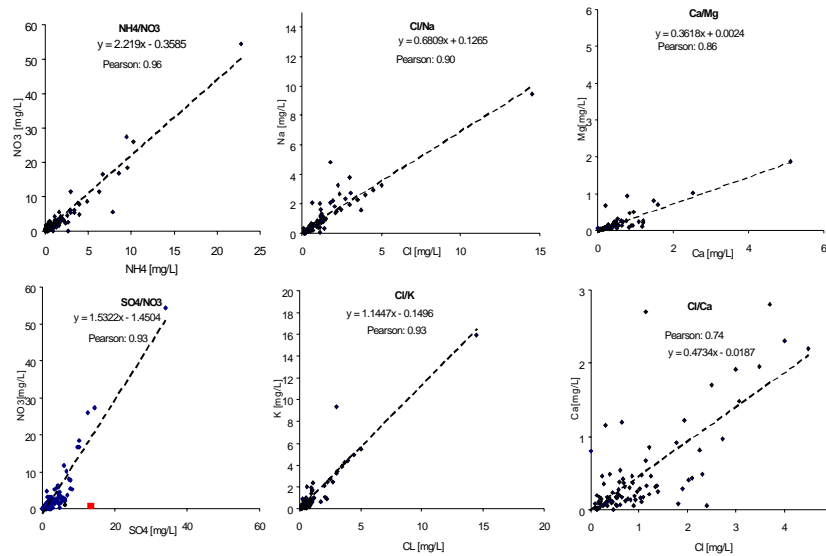
Fig. 6. Correlation plots for normalized ion concentrations NH_4/NO_3 and NH_4/SO_4 (left), Cl/Na and Cl/K (middle), Ca/Mg and Ca/Cl (right).
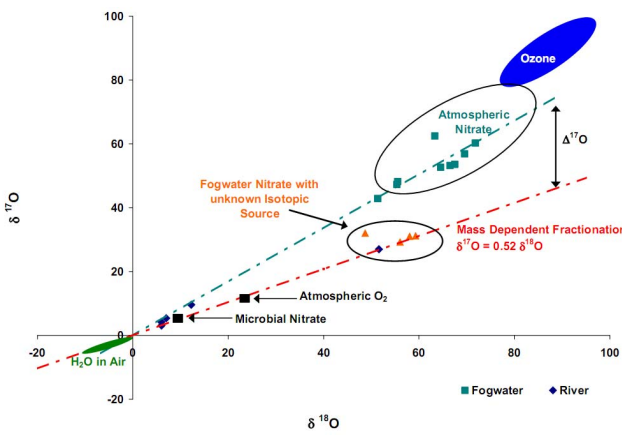

Fig. 7. Oxygen triple isotope plots for nitrate in 14 fogwater and 5 river water samples.

Fig. 8. 10-days back trajectories for sample #15 (see text for further information).

trajectories of those two days only which contributed most fog water to the weekly samples.

3.3 Ca, Mg, and PO$_4$ (Fig. 5)

Figure 5 shows analoguous ion plots for Ca, Mg, and PO$_4$ as analysed from the El Tiro weekly fog samples. Like in the Figs. 3 and 4, the five characteristic peaks are marked by numbers.

Ca and Mg are thought to originate from dust sources (Formenti et al., 2001; Roberts et al., 2001), and the significant Pearson correlation coefficient of 0.86 (Fig. 6) we find for normalized Ca/Mg ion concentrations confirms the common source. With 2.76 the Ca/Mg ratio is slightly higher than
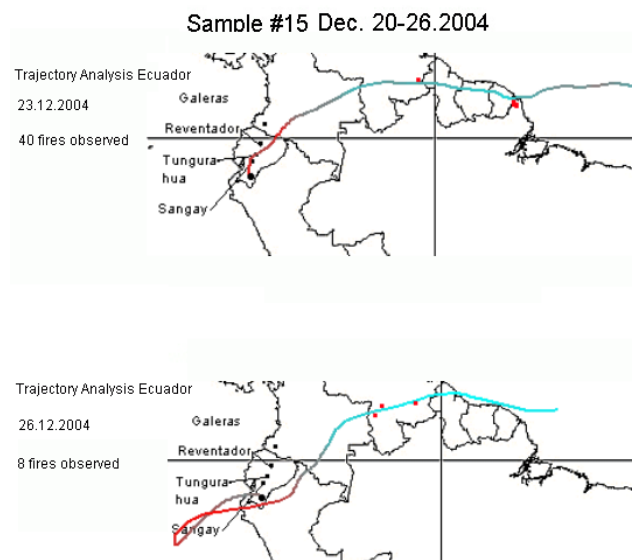
2.0 found by Boy and Wilcke (2008) at the same research site. The back trajectories shown in Figs. 9–12 related to the peaks #42, 46, 62, and 73 all point to dust sources in North Africa. In fact, aerosol index images from the Ozone Monitoring Instrument (OMI) aboard a NASA satellite clearly show outbursts of Sahara dust during these periods which are transported rapidly over the Atlantic Ocean right into South America. According to Koren et al. (2006) the Sahara is the main supplier of mineral dust to the Amazon. OMI aerosol index images show that around the equinoxes mineral dust
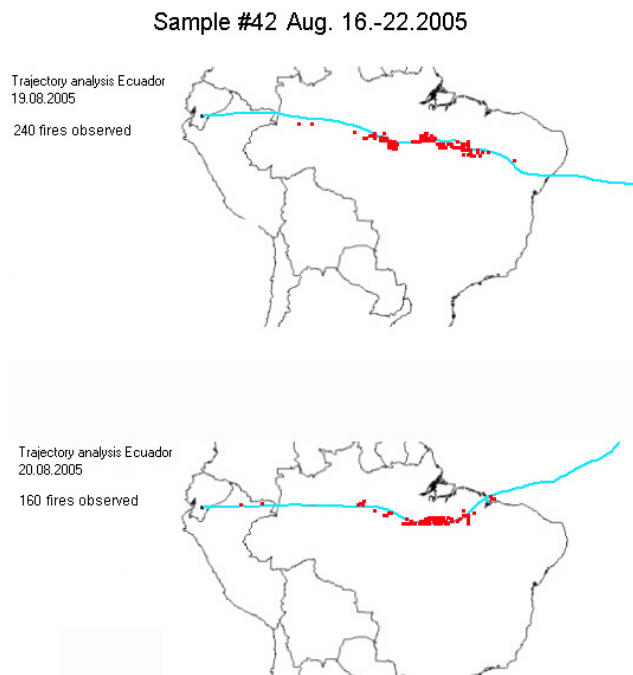
Sample #42 Aug. 16.-22.2005

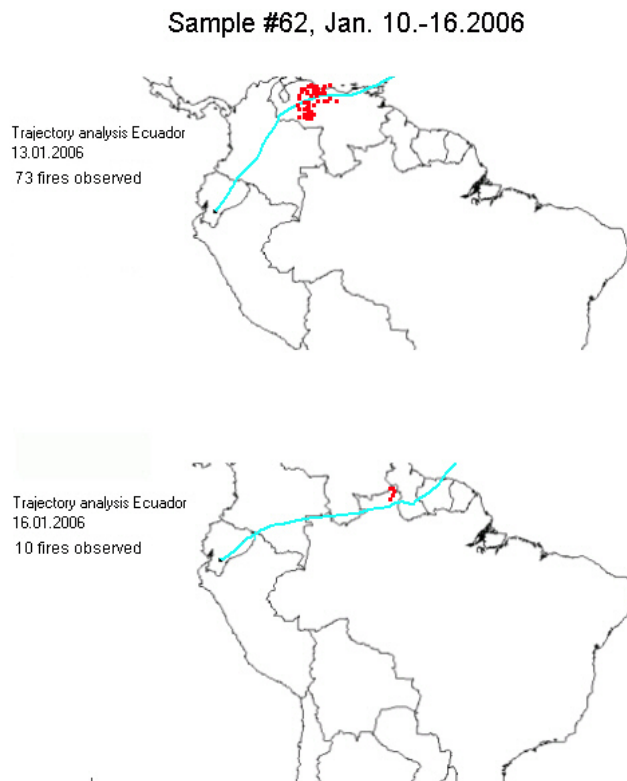Trajectory analysis Ecuador
19.08.2005

240 fires observed

Trajectory analysis Ecuador
20.08.2005

160 fires observed

Fig. 9. Same as Fig. 8, but for sample #42.

Sample #46, Sep. 6.-11.2005

Trajectory analysis Ecuador
08.09.2005

166 fires observed

Trajectory analysis Ecuador
11.09.2005

3 fires observed

Fig. 10. Same as Fig. 8, but for sample #46.

Sample #62, Jan. 10.-16.2006

Trajectory analysis Ecuador
13.01.2006

73 fires observed

Trajectory analysis Ecuador
16.01.2006

10 fires observed

Fig. 11. Same as Fig. 8, but for sample #62.

Sample #73 Mar. 7.-13.2006

Trajectory analysis Ecuador
09.03.2006

7 fires observed

Trajectory analysis Ecuador
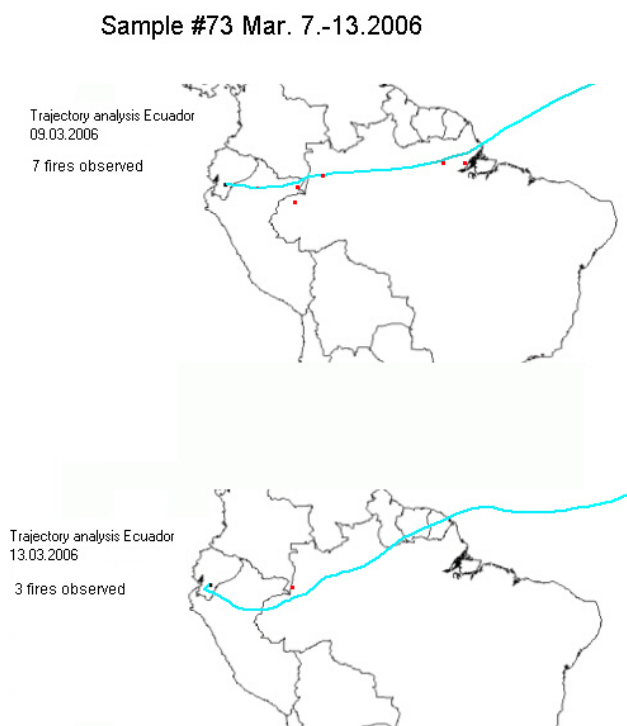13.03.2006

3 fires observed

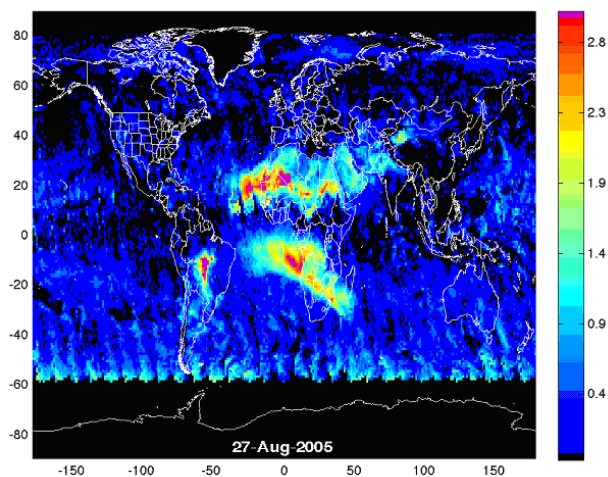**Fig. 12.** Same as Fig. 8, but for sample #73.

Fig. 13. 3-day averaged OMI aerosol index (AI) map showing distinct regions of aerosol outflow from Africa towards South America. The data were obtained from NASA/GSFC TOMS server (ftp://toms.gsfc.nasa.gov/pub/omi/data/aerosol/) processed in Matlab. Averaging of data was done to smoothen image quality.

from both the NH deserts (Sahara) as well as from SH deserts (Namib) can be identified to reach into the South American tropics. An example is given in Fig. 13.

It is interesting to note that the correlation between Cl and Ca normalized ion concentrations yields a Pearson correlation coefficient as high as 0.74 (Fig. 6). If it is accepted that Ca originates from African dust sources the uptake of oceanic compounds over the Atlantic is plausible.

PO_4 shows only 5 significant peaks for the 3 years period discussed here. The most prominent ones are peaks #62 and #73. For both samples respective back trajectories point to North African sources. Indeed, phosphate mining is undertaken in Marocco, Tunisia and in the Western Sahara. Although Mahowald et al. (2005) argue that biomass burning may be a significant source of phosphorus, phosphate mining in North Africa appears to be the main source of the PO_4 found in our Ecuadorian fog samples. Figure 14 shows characteristic back trajectories for all PO_4 peaks of our data series. With 2 exceptions related to peaks #53 and 57, with air from the Pacific coast off Peru (Guano?), all other trajectories originate in or near North Africa.

4   Concluding remarks

Annual depositions of major nutrients into the mountaineous rain forest in South Ecuador, by rain and fog, have been quantified based on 5 years of regular sampling.

Most of the Na, Cl, and K as well as Ca and Mg input from oceanic and desert dust sources, respectively, is natural. PO_4 may have natural biogenic sources, but from our study phosphate mining is likely to be the dominating (anthropogenic) source.
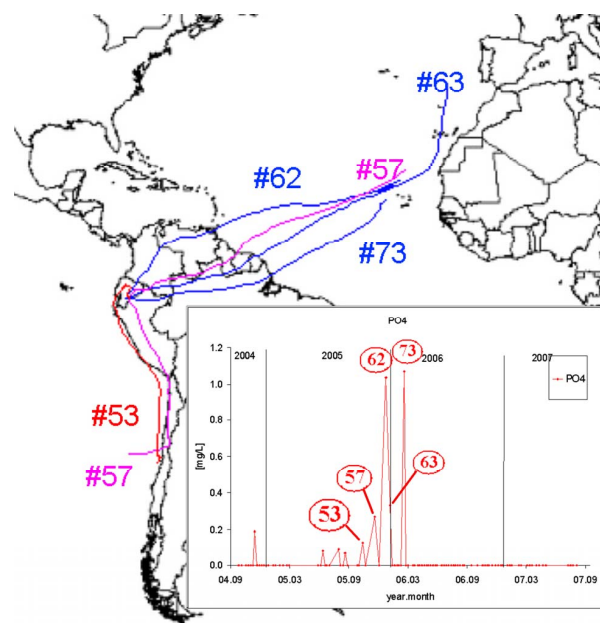

Fig. 14. 10-days back trajectories for dominant PO_4 peaks which are also shown.

NO_3, NH_4, and most of SO_4 (about 90%) are almost entirely due to anthropogenic sources, most likely biomass burning. Industrial and transportation emissions and other pollutants may act in a similar way as the precursors produced by biomass burning. Their contribution is unknown at present. We hope to clarify this aspect by an ongoing study using new emission inventories for South America.

About 10% of the observed SO_4 deposition is likely to originate from active volcanoes in Ecuador.

The mountaineous rain forest in Ecuador has developed on poor acidic soil, with a low rate of mineralization. It is virtually fertilized by nutrients carried in by rain and fog. The significant input of sulfate, ammonia and nitrate, at a rate common in polluted central Europe, from anthropogenic sources, is a disturbance which might have an impact on this ecosystem and its biodiversity. Ongoing controlled fertilizing experiments in parts of this Ecuadorian research site aim at investigating the likely effect of this anthropogenic disturbance.

Edited by: R. Garraud
Reviewed by: one anonymous referee

References

Andreae, M. O., Talbot, R. W., Berresheim H., and Beecher, K. M.: Precipitation chemistry in Central Amazonia, J. Geophys. Res., 95, 16987–16999, 1990.

Andreae, M. O. and Merlet, P.: Emission of trace gases and aerosols from biomass burning, Global Biogeochem. Cy., 15, 955–960, 2001.

Andreae, M. O., Artaxo, P., Fischer, H., Freitag, S. R., Gregoire, J.-M., Hansel, A., Hoor, P., Kormann, R., Krejci, R., Lange, L., Lelieveld, J., Lindinger, W., Longo, K., Peters, W., deReus, M., Scheeren, B., Silvia Dias, M. A. F., Ström, J., van, Velthoven, P. F. J., and Williams, J.: Transport of biomass burning smoke to the upper troposphere by deep convection in the equatorial region, Geophys. Res. Lett., 28, 951–954, 2001.

Andreae, M. O., Rosenfeld, D., Artaxo, P., Costa, A. A., Frank, G. P., Longo, K. M., and Silva Dias, M. A. F.: Smoking rain clouds over the Amazon, Science, 303, 1337–1342, 2004.

Artaxo, P., Maenhaut, W., Storms, H., and van Grieken, R.: Aerosol characteristics and sources for the Amazon basin during the wet season, J. Geophys. Res., 95, 16971–16985, 1990.

Ashbury, C. E., McDowell, W. H., Trinidad-Pizarro, R., Berrios, S.: Solute deposition of a Puerto Rican montane forest, Atmos. Environ., 28, 1773–1780, 1994.

Boj, J., Rollenbeck, R., Valarezo, C., and Wilcke, W.: Amazonian biomass burning-derived acid and nutrient deposition in the north Andean montane forest of Ecuador, Global Biogeochem. Cy., 22, GB4011, doi:10.1029/2007GB003158, 2007.

Boy, J. and Wilcke, W.: Tropical Andean forest derives calcium from Saharan dust, Global Biogeochem. Cy., 22, GB1027, doi:10.1029/2007GB002960, 2008.

Chang, J. S., Brost, R. A., Isaksen, I. S. A., Madronich, S., Middleton, P., Stockwell, W. R., and Walcek, C. J.: A three-dimensional Eulerian acid deposition model:Physical concepts and formulation, J. Geophys. Res., 92, 14681–14700, 1987.

Clark, K. L., Nadkerni, N. M., Schaefer, D. R., and Gholz, W. L.: Cloud water and precipitation chemistry in a tropical mountain forest, Montaverde, Costa Rica, Atmos. Environ., 32, 1595–1603, 1998.

Crutzen, P. J. and Andreae, M. O.: Biomass burning in the tropics: Impact on atmospheric chemistry and biogeochemical cycles, Science, 250, 1669–1678, 1990.

Cuevas, E. and Medina, E.: Nutrient dynamics within Amazonian forests I. Nutrient flux in fine litter fall and efficiency of nutrient utilization, Oecologia, 68, 466–472, 1986.

Cuevas, E. and Medina, E.: Nutrient dynamics within Amazonian forests II. Fine root growth, nutrient availability and litter decomposition, Oecologia, 76, 222–235, 1988.

Damoah, R., Spichtinger, N., Forster, C., James, P., Mattis, I., Wandinger, U., Beirle, S., Wagner, T., and Stohl, A.: Around the world in 17 days – hemispheric-scale transport of forest fire smoke from Russia in May 2003, Atmos. Chem. Phys., 4, 1311–1321, 2004,
http://www.atmos-chem-phys.net/4/1311/2004/.

Fabian, P., Kohlpaintner, M., and Rollenbeck, R.: Biomass Burning in the Amazon – Fertilizer for the Mountaineous Rain Forest in Ecuador, Environ. Sci. Pollut. Res., 12, 290–296, 2005.

Formenti, P., Andreae, M. O., Lange, L., Roberts, G., Cafmeyer, J., Rajta, I., Maenhaut, W., Holben, B. N., Artaxo, P., and Lelieveld, J.: Saharan dust in Brazil and Suriname during the large-scale biosphere-atmosphere experiment in Amazonia (LBA)-cooperative LBA regional experiment (CLAIRE) in March 1998, J. Geophys. Res., 106(D14), 14919–14934, 2001.

Fujiwara, M., Kita, K., Kawakami, S., Ogawa, T., Komela, N., Saraspinya, S., and Surigsto, A.: Tropospheric ozone enhancements during the Indonesian fire events in 1994 and 1997 as revealed by ground-based observations, Geophys. Res. Lett., 26, 2417–2420, 1999.

Graham, B., Guyon, P., Maenhaut, W., Taylor, P. E., Ebert, M., Matthias-Maser, S., Mayol-Bracaro, O. L., Godoi, R. H. M., Artaxo, P., van Grieken, R., Glovsky, M. M., Flagan, R. C., and Andreae, M. O.: Composition and diurnal variability of the natural Amazonian aerosol, J. Geophys. Res., 108(D24), 4765–4783, doi:10.1029/2003JD004049, 2003.

Koren, I., Kaufman, Y. J., Remer, L. A., and Marius, J. V.: Measurement of the effect of Amazon smoke on inhibition of cloud formation, Science, 303, 342–345, 2004.

Koren, I., Kaufman, Y. J., Washington, R., Todd, M. C., Rudich, Y., Martins, J. V., and Rosenfeld, D.: The Bode'le depression:a single spot in the Sahara that provides most of the mineral dust to the Amazon forest, Environ. Res. Lett., 1, 01405, doi:10.1088/1748-9326/1/1/014005, 2006.

Mahowald, N. M., Artaxo, P., Baker, A. R., Jickells, T. D., Okin, G. S., Gregory, S., Randerson, J. T., and Townsend, A. R.: Impacts of biomass burning emissions and landuse change on Amazonian atmospheric phosphorus cycling and deposition, Global Biogeochem. Cy., 19, GB4030, doi:10.1029/2005GB002541, 2005.

Marufu, L., Dentener, F., Lelieveld, J., Andreae, M. O., and Helas, G.: Photochemistry in the African troposphere:influence of biomass burning emissions, J. Geophys. Res., 105, 14513–14530, 2000.

Roelofs, G.-J., Lelieveld, J., Smit, H. G., and Klug, D.: Ozone production and transport in the tropical Atlantic region during the biomass burning season, J. Geophys. Res., 102, 10637–10651, 1997.

Rollenbeck, R., Fabian, P., and Bendix, J.: Precipitation dynamics and chemical properties in tropical mountain forests of Ecuador, Adv. Geosci., 6, 73–76, 2006,
http://www.adv-geosci.net/6/73/2006/.

Rollenbeck, R., Bendix, J., Fabian, P., Boy, J., Dalitz, H., Emck, P., Oesker, M., and Wilcke, W.: Comparison of different techniques for the measurement of precipitation in tropical montane rain forest regions, J. Atmos. Ocean. Tech., 24, 156–168, 2007.

Schemenauer, R. and Cereceda, P.: A proposed standard fog collector for use in high-elevation regions, J. Appl. Meteorol., 33, 1313–1322, 1994.

Spichtinger, N., Wenig, M., James, P., Wagner, T., Platt, U., and Stohl, A.: Satellite detection of a continental-scale plume of nitrogen oxides from boreal forest fires, Geophys. Res. Lett., 28, 4579–4582, 2001.

Stohl, A. and Wotawa, G.: A method for computing single trajectories representing boundary layer transport, Atmos. Environ., 29, 3235–3239, 1995.

Talbot, R. W., Andreae, M. O., Berresheim, H., Artaxo, P., Garstang, M., Harriss, R. C., Beecher, K. M., and Li, S. M.: Aerosol chemistry during the wet season in Central Amazonia: The influence of long-range transport, J. Geophys. Res., 95, 16955–16969, 1990.

Tanimoto, H., Kaji, Y., Hirokawa, J., Akimoto, H., and Minko, N.
    P.: The atmospheric impact of boreal forest fires in far eastern
    Siberia on the seasonal variation of carbon monoxide: Observa-
    tions at Rishiri, a northern remote island in Japan, Geophys. Res.
    Lett., 27, 4073–4076, 2000.

Thiemens, M. H.: History and applications of mass-independent
    isotope effects, Annu. Rev. Earth Planet. Sci., 34, 217–262, 2006.
Veneklaas, E. J.: Nutrient fluxes in bulk precipitation and through-
    fall in two montane tropical rain forests, Colombia, J. Ecol., 78,
    974–992, 1990.